9, 643 (1971); hereafter to be referred to as I.
[7]R. H. Parmenter, Phys. Rev. 100, 573 (1955).
[8]D. Brust, Phys. Rev. 134, A1337 (1964).
[9]J. Walter and M. L. Cohen, Phys. Rev. 183, 763 (1969).
[10]J. C. Phillips, in Ref. 2, Vol. 18, pp. 55–164.
[11]W. J. Choyke, D. R. Hamilton, and Lyle Patrick, Phys. Rev. 133, A1163 (1964).
[12]B. E. Wheeler, Solid State Commun. 4, 173 (1966).
[13]W. J. Choyke and L. Patrick, Phys. Rev. 187, 1041 (1969).
[14]M. L. Belle, N. K. Prokof'eva, and M. B. Reifman, Sov. Phys. Semicond. 1, 315 (1967).
[51]F. Herman, J. P. Van Dyke, and R. L. Kortum, Mater. Res. Bull. 4, S167 (1969).
[16]P. J. Gielisse, S. S. Mitra, J. N. Plendl, R. D. Griffis, L. C. Mansur, R. Marshall, and E. A. Pascoe, Phys. Rev. 155, 1039 (1967).
[17]J. C. Phillips, Rev. Mod. Phys. 42, 317 (1970); J. A. Van Vechten, Phys. Rev. 182, 891 (1969); 187, 1007 (1969).
[18]V. A. Fomichev, I. I. Zhukova, and I. K. Polushina, J. Phys. Chem. Solids 29, 1025 (1968).
[19]C. C. Wang, M. Cardona, and A. G. Fischer, RCA Rev. 25, 159 (1964).
[20]H. Philipp and E. A. Taft, Phys. Rev. 127, 159 (1962).
[21]J. C. Phillips, J. Chem. Phys. 48, 5740 (1968).
[22]V. A. Fomichev and M.A. Rumsch, J. Phys. Chem. Solids 29, 1015 (1968).
[23]Reported as a private communication in the paper on the energy bands of BN, D. R. Wiff and R. Keown, J. Chem. Phys. 47, 3113 (1967).
[24]L. Kleinman and J. C. Phillips, Phys. Rev. 117, 460 (1959).
[25]F. Bassini and M. Yoshimine, Phys. Rev. 130, 20 (1963).

PHYSICAL REVIEW B VOLUME 6, NUMBER 4 15 AUGUST 1972

Optic Modes in Amorphous As_2S_3 and As_2Se_3

G. Lucovsky
Xerox Palo Alto Research Center, Palo Alto, California 94304
(Received 27 March 1972)

New reflectance spectra are obtained for amorphous As_2S_3 and As_2Se_3. The spectra contain features not reported in earlier studies. Analysis of the spectra in terms of damped Lorentzian oscillators, combined with new Raman data, gives further support to the validity of a molecular model for the optic-mode vibrational frequencies. Using mode masses derived from the model, values of the macroscopic effective charge e_T^* are obtained. For both materials, e_T^* values are comparable to those of other covalently bound solids; e.g., trigonal Se and trigonal Te. Contrary to early suggestions, it is demonstrated that the large values of e_T^* in these materials are not a manifestation of ionic bonding but rather result from dynamical charge transfer. In both As_2S_3 and As_2Se_3 there are sufficient differences between the infrared (ir) and Raman spectra so that they cannot be interpreted simply in terms of a density of states by assuming a complete breakdown of selection rules due to disorder. On the contrary, selection rules resulting from the short-range order or the molecular nature of these solids are of considerable importance in determining the ir or Raman activity of the optic modes.

I. INTRODUCTION

The first report of reststrahlen bands in chalcogenide glasses was made by Hilton *et al.*[1] Felty, Lucovsky, and Myers[2] studied the dominant reststrahlen band in both As_2S_3 (at ~300 cm^{-1}) and As_2Se_3 (at ~220 cm^{-1}) and found that this band displayed a two-mode behavior[3] in the pseudobinary alloy system $As_2S_{3-x}Se_x$ analogous to that reported for crystalline alloy systems, e.g., $CdS_{1-x}Se_x$. Taylor, Bishop, and Mitchell[4] studied As_2Se_3 in greater detail. They identified a second and weaker reststrahlen (at ~100 cm^{-1}) and studied the absorption spectrum as well. They found that a Gaussian line shape gave a better fit to the wings of the absorption bands than did a Lorentzian line shape. Infrared (ir) reflectance bands in crystalline materials have traditionally been fit with damped Lorentzian oscillators. Zlatkin and Markov[5] studied both crystalline and amorphous As_2S_3 and As_2Se_3. They calculated values of the Szigeti effective charge e_s^* for the amorphous materials and suggested that the large values of e_s^* they found, $0.94e$ for As_2S_3 and $0.67e$ for As_2Se_3, were indicative of a substantial ionic content to the chemical bonding. Onomichi, Arai, and Kudo[6] also studied amorphous As_2S_3 and As_2Se_3 and reported similar values for e_s^*. The Raman spectrum of As_2S_3 was studied by Ward and Myers[7] and by Kobliska and Solin[8] and that of As_2Se_3 by Schottmiller *et al.*[9] A comparison of the ir and Raman data indicated that the frequencies of the dominant modes are different.[10]

In this paper we present new reflectance spectra for As_2S_3 and As_2Se_3 in the region of the dominant reststrahlen bands, 180–450 cm^{-1}. In the earlier

work,[2,4] these reststrahlen bands were fit with a single Lorentzian oscillator; our data, done in higher resolution, can only be fit with two oscillators. For As_2S_3, the second and newly identified oscillator coincides in frequency and half-width with the dominant Raman mode as observed in a symmetric scattering geometry.[8] We have also measured the transmission spectrum of As_2Se_3. The values of the absorption constant from our transmittance measurements are in close agreement with those calculated from the oscillator parameters of the reflectance fit.

Austin and Garbett[11] noted similarities between the optic-mode frequencies of As_2Se_3 and $AsBr_3$ and suggested that a molecular approach similar to that followed by Bell and co-workers[12] on fused silica (SiO_2) would be appropriate for these materials. In a parallel effort, Lucovsky and Martin[13] developed a molecular model for the optic modes in chalcogenide glasses, applied the model to As_2S_3 and As_2Se_3, and demonstrated excellent agreement between their calculated optic-mode frequencies and those reported in the literature. We are here conerned with effective charges which are a measure of the strength of the infrared-active optic modes. A calculation of the effective charges from the optical data requires a knowledge of the atomic motions of the optic modes in order to calculate a mode mass. Using the molecular model,[13] we are able to assign mode masses and calculate effective-charge parameters. These are tabulated for both As_2S_3 and As_2Se_3. It is well known that there are both static (ionic) and dynamic contributions[14] to the infrared effective charge. In this paper we use e_T^*, the macroscopic effective charge,[15] rather than the Szigeti charge e_s^*. These two charges are simply related through the optical frequency dielectric constant ϵ_0:

$$e_T^* = \tfrac{1}{3}(\epsilon_0 + 2)\, e_s^* \,. \qquad (1)$$

Zlatkin and Markov[5] suggested that the strong reststrahlen in As_2S_3 and As_2Se_3 were evidence of strong ionic contributions to the chemical bonding. This is not necessarily correct. There are examples of strong reststrahlen, with comparable effective charges, in ionic materials NaCl, KCl, etc., in covalent semiconductors GaAs, GaP, etc., as well as in homopolar materials trigonal Se and Te.[14] For the last two materials, there is no static or ionic contribution to the effective charge. All of the contributions are dynamic with the dominant mechanism being one of charge displacement during the optic-mode motion.[14]

We apply the molecular model of Lucovsky and Martin[13] and obtain estimates of e_T^* for As_2S_3 and As_2Se_3 for two limiting cases. One estimate is made for a rigid-ion model in which the bonding is assumed to be ionic. In this model, e_T^* is approximately equal to the static ionic charge. The second estimate for e_T^* is based on a model in which the bonding is covalent. In this case the effective charge is dynamic and is associated with charge redistribution (or deformation). The values of e_T^* we obtain from the analysis of the reflection data can only be reconciled with a model in which the dominant contributions to e_T^* are dynamic, and due to a redistribution of charge between neighboring bonds which are alternatively under compression and tension.[10]

II. EXPERIMENTAL TECHNIQUES

The infrared reflectance and transmittance measurements were made using two instruments, a Perkin Elmer 180 spectrometer for the frequency range 180–600 cm^{-1} and a Hitachi FIS 3 spectrometer for the range 60–400 cm^{-1}. Both instruments were operated in a double-beam mode; for the reflectance measurements, the sample reflectance was compared with that of an Al mirror. Reflectance spectra were run at room temperature on three samples of As_2S_3; these were obtained from Servo Corporation. Reflectance spectra were also run on two samples of As_2Se_3; these were cut from bulk quenched ingots. Absorption measurements were also made on thin films of As_2Se_3; the films were prepared by vapor deposition. Film thickness was monitored by a quartz crystal oscillator technique; film composition was determined by x-ray fluorescence analysis.

Our emphasis in this work is on the dominant reststrahlen bands; these occur at ~300 cm^{-1} in As_2S_3 and at ~210 cm^{-1} in As_2Se_3. Figure 1 shows the reflectance spectra of As_2S_3 and As_2Se_3 in the frequency range 180–500 cm^{-1}. These spectra were recorded at higher resolution, ~2 cm^{-1}, than those of earlier workers[1,2,5] and show considerable fine structure on the high-frequency side of the reststrahlen bands. For As_2S_3, the structure consists of a distinct minimum at ~400 cm^{-1}, and two inflections, at 330 and 375 cm^{-1}. For As_2Se_3, the corresponding structure occurs at 280, 235, and 250 cm^{-1}. The fine structure was present in all of the As_2S_3 and As_2Se_3 samples studied and was not identified in earlier studies. In at least one of these studies,[2] spectra were recorded using single-beam techniques in which variations in the operating parameters, between sample and reference runs, were apparently sufficient to obliterate the structure. Also shown in Fig. 1 are oscillator fits to the reflectance[16]; the oscillator-fit parameters are given in Table I. The parameters were obtained by means of a computer program which performs an iterative search in parameter space. The optimization criterion was a minimization of the rms deviation of the synthesized reflectance from the experimental reflectance. Three oscillators

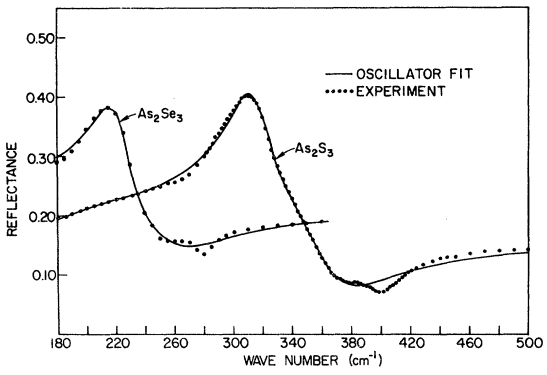

FIG. 1. Room-temperature reflectance spectra of amorphous As_2S_3 and As_2Se_3. Circles represent experimental data; the solid lines designate spectra synthesized from damped Lorentzian oscillators.

were used for each material. Two of these are for the spectral region shown and one for a weaker low-frequency band, at ~ 160 cm^{-1} in As_2S_3 and at ~ 100 cm^{-1} in As_2Se_3. For As_2S_3, the resultant rms deviation was 0.006; for As_2Se_3, also 0.006. An attempt to fit the reflectance using only one oscillator for the dominant reststrahlen yielded poorer fits, particularly in the vicinity of the leading edge of the band where the fine structure occurs. For the two oscillator fits, the corresponding rms deviations are 0.014 for As_2S_3 and 0.012 for As_2Se_3.

Figure 2 contains a plot of the absorption spectrum of As_2Se_3 in the frequency range 180–300 cm^{-1}. The experimental values are obtained by measuring the transmission spectrum on samples of different thicknesses. The calculated values are obtained from the oscillator fit to the reflectance. The agreement is quite good. Taylor, Bishop, and Mitchell[4] also studied the absorption spectrum of As_2Se_3. They found that the main absorption band, near 220 cm^{-1}, was better fit with a Gaussian line shape with a center frequency of 237 cm^{-1} than with a Lorentzian line. We have demonstrated that the absorption and reflectance spectra can be fit with two Lorentzian modes. We also find evidence of a third and weaker mode at ~ 275 cm^{-1}. There is nothing in our experimental data that favors a Gaussian line shape.

TABLE I. Oscillator fit parameters.

Material	Oscillator parameters: Frequency ω_i (cm^{-1})	Strength $S_i = \Delta\epsilon_i$	Damping constant γ_i	Phonon frequencies (cm^{-1}): $\omega_{TO}(i)$	$\omega_{LO}(i)$
As_2S_3	163	0.48	0.15	163	167
	309	0.98	0.09	309	336
	340	0.44	0.17	340	358
As_2Se_3	101	0.70	0.19	101	105
	218	1.17	0.11	218	237
	246	0.38	0.23	246	255

III. DIELECTRIC DISPERSION PROPERTIES

Figure 3 contains plots of the frequency dependence of ϵ_2, the imaginary part of the complex dielectric constant $\epsilon = \epsilon_1 + i\epsilon_2$, and of the energy-loss function, $-\mathrm{Im}(\epsilon^{-1})$ for As_2S_3. Figure 4 contains the same plots for As_2Se_3. The position of the peaks in ϵ_2 locate the frequencies of the transverse optical (TO) phonons, and the peaks in $-\mathrm{Im}(\epsilon^{-1})$ locate the frequencies of the longitudinal optical (LO) phonons. These are also contained in Table I.

Figure 5 contains plots of effective densities of states as derived from the Raman and ir studies for As_2S_3. The Raman density of states is deduced from the data of Kobliska and Solin[8] who used a data-reduction scheme outlined by Shuker and Gammon.[17] The Raman density of states is obtained for a scattering geometry in which the incident and scattered polarizations are parallel. Unpublished data of Kobliska and Solin[18] give a peak in $\rho_{eff}(R)$ at lower frequencies (~ 315 cm^{-1}) for a scattering geometry in which the polarization vectors of the incident and scattering light are at an angle of 90 deg. For the infrared effective density of states $\rho_{eff}(\mathrm{ir})$, we have plotted $\omega^2\epsilon_2$, as derived from our oscillator fit. In addition to plotting the total $\omega^2\epsilon_2$, we have plotted the individual contributions due to the modes at 309 and 340 cm^{-1}. This decomposition of $\rho_{eff}(\mathrm{ir})$ into its constituent lines demon-

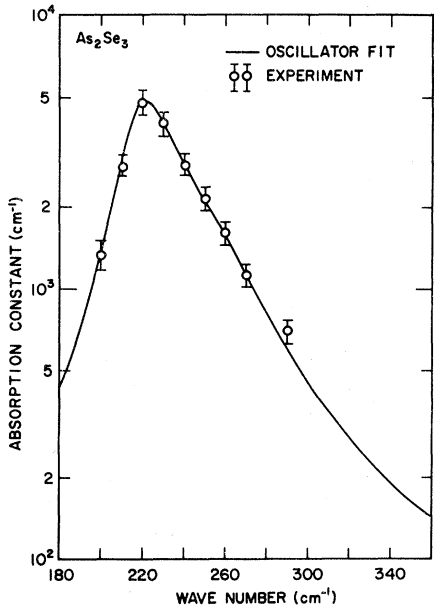

FIG. 2. Room-temperature absorption constant vs frequency for As_2Se_2. Open circles represent values derived from an analysis of the transmission spectra of thin films. The solid line is the absorption constant as derived from the parameters of the oscillator fit.

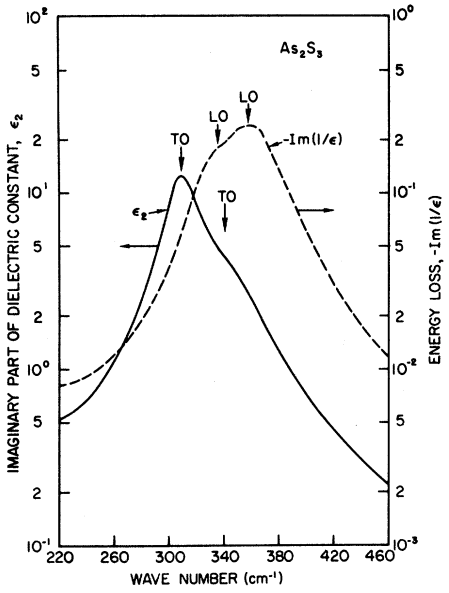

FIG. 3. Dielectric dispersion properties of amorphous As_2S_3: ϵ_2 is the imaginary part of the dielectric constant; $-\mathrm{Im}(1/\epsilon)$ is the energy-loss term. Also shown are the frequencies of the transverse-optic (TO) and longitudinal-optic (LO) modes.

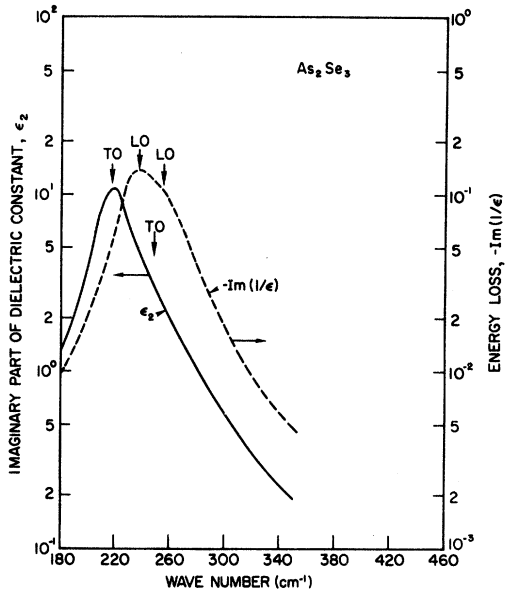

FIG. 4. Dielectric dispersion properties of amorphous As_2Se_3: ϵ_2 is the imaginary part of the dielectric constant; $-\mathrm{Im}(1/\epsilon)$ is the energy-loss term. Also shown are the frequencies of the transverse-optic (TO) and longitudinal-optic (LO) modes.

strates that the mode observed in Raman scattering by Kobliska and Solin[8] is also ir active. The shift of the Raman peak with scattering geometry suggests that there is Raman activity in the mode at 309 cm^{-1} as well. The totality of measurements suggests a symmetric mode at 340 cm^{-1} and an antisymmetric mode at 309 cm^{-1}.

A controversy as to whether there are one or two modes in As_2Se_3 in the vicinity of the dominant ir and Raman bands arose because of the analysis of the absorption data by Taylor, Bishop, and Mitchell.[3,19] They fit their absorption data with a Gaussian line centered at 237 cm^{-1}; the Raman data of Schottmiller *et al.* gave a single band at 227 cm^{-1} and it was suggested that these were one and the same mode. Our analysis of the reflectance yields two Lorentzian modes for As_2Se_3 in this frequency region, one at 218 cm^{-1} and one at 246 cm^{-1}. The results we have presented here for As_2S_3 also clearly indicate that there are two modes in the dominant reststrahlen region. Furthermore, the Raman scattering results of Kobliska and Solin,[7,17] as well as new Raman scattering experiments on As_2Se_3 by Ward,[20] also identify two modes in this region. In our subsequent tables we therefore quote frequencies that are derived from our ir measurements, rather than the data of Ref. 4.

IV. MOLECULAR MODEL

One of our primary concerns in this paper is a determination of the effective charges associated with the infrared-active modes and the identification of the mechanism that is responsible for the ir activity. The effective-charge parameter we will use is the macroscopic effective charge e_T^*,[21] defined by

$$e_T^* = \left(\frac{\partial M}{\partial u}\right)_E , \tag{2}$$

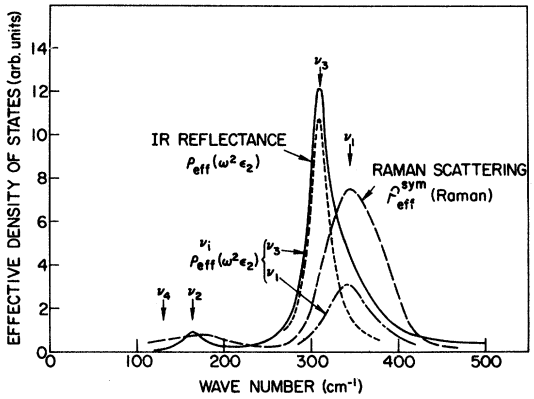

FIG. 5. Infrared and Raman effective density of states of As_2S_3. The infrared density of states is given by $\omega^2\epsilon_2$, derived from the oscillator fit. The Raman density of states is obtained from a reduction of experimental data (Ref. 8) using the procedure outlined by Shuker and Gammon (Ref. 17); polarizations of the incident and scattered light are parallel. The frequency markers ν_i, $i=1$, 2, 3, 4, identify frequencies calculated from the molecular model of Lucovsky and Martin (Ref. 13).

where M is the first-order (linear) electric moment induced by the relative (or optical) displacements of the atoms, u is the relative atomic displacement coordinate, and E is the macroscopic electric field, which is identically equal to zero for TO phonons. The effective charge can be calculated from the strength of the infrared mode, S_i $(=\Delta\epsilon_1^i)$, as determined through the oscillator fit. $\Delta\epsilon_1^i$ is the contribution to the real part of the dielectric constant for the ith mode. ϵ is the complex dielectric constant,

$$\epsilon = \epsilon_0 + \sum_i [S_i \omega_i / (\omega_i^2 - \omega^2 - i\gamma_i \omega\omega_i)] , \quad (3)$$

where ϵ_0 is the optical frequency dielectric constant, ω_i is the TO phonon frequency of the ith mode, and γ_i is a damping constant. e_T^* is then given by

$$e_T^* = \pi^{1/2} c m_i^{1/2} S_i^{1/2} \nu_i / N^{1/2} , \quad (4)$$

where ν_i is the TO phonon frequency (in wave numbers), N is the number of oscillators per unit volume, c is the velocity of light, and m_i is the mode mass. The mode mass is determined by considering the atomic motions and equating them to an equivalent oscillating dipole. It is this parameter that we determine through a molecular model for the optic-mode atomic displacements.

Lucovsky and Martin[13] have developed a model for calculating the optic-mode frequencies of molecular amorphous solids and have applied it to the chalcogenide glasses, As_2S_3 and As_2Se_3. The calculation is based on the identification of a structural unit which exemplifies the short-range order of the atomic constituents of the glass. The applicability of such a model ultimately rests on a weak coupling between the molecular units. For example, for fused silica (SiO_2), the molecular unit is an SiO_4 tetrahedron. The calculations of Bell and co-workers[12] and of Su and Bock[22] indicate that in that structure weak coupling occurs at the bridging oxygen atoms. Specifically, the bond-bending force constant at the bridging oxygen atoms in SiO_2 is an order of magnitude smaller than the bond-bending force constant at the Si atoms (O-Si-O) and two orders of magnitude smaller than the Si-O bond-stretching force constant. A similar behavior occurs in fused germania (GeO_2).[23] The structural units in the model for As_2S_3 and As_2Se_3 are, respectively, pyramidal AsS_3 and $AsSe_3$ molecules. Figure 6 is a schematic representation of the structural model for As_2S_3. The local order is essentially the same as that of the crystalline phase of As_2S_3, orpiment.[24] The pyramidal bonding configuration about the As atoms also occurs in the gaseous molecules $AsCl_3$, $AsBr_3$, and AsI_3[25]; the bonding geometry at the bridging S sites is typical of S-S bonding in elemental forms of S and in other compounds; e.g., organo-S systems. In applying the molecular model we assume that the bond-bending force constants at the bridging S and Se atoms, respectively, in As_2S_3 and As_2Se_3 are relatively weak, i.e., that the behavior at these bridging chalcogenide atoms is similar to that at the O sites in SiO_2 and GeO_2.

Table II contains a comparison of the calculated and experimentally determined optic-mode frequencies. In the Lucovsky-Martin work,[13] the authors considered all of the modes of the system; here we focus only on the dominant modes which are associated with the pyramidal molecules. Weaker structure occurs in the ir spectra, and it has been demonstrated that this structure can be understood in terms of the weaker intermolecular coupling,[13] e.g., in terms of the optic-mode frequencies of bent triatomic chains, As-S(Se)-As. The calculated frequencies for As_2S_3 and As_2Se_3, respectively, were obtained by scaling the frequencies of the molecules $AsCl_3$[25] and $AsBr_3$.[26] The scale factors were established on the basis of a comparison of the frequencies of the dominant Raman modes. The frequencies of the other modes then follow from the near equivalence of the respective mass ratios

$$m_{As}/m_{S\,(Se)} \approx m_{As}/m_{Cl(Br)} \quad (5)$$

and the force constant ratios k_δ/k_r. m_j is the atomic mass of the jth atomic species, (j = As, S, Se, Cl, Br), k_δ is the bond-bending force constant at the As atoms, and k_r is the bond-stretching force constant. Within the framework of a valence-force-field calculation, the frequency of the ith mode can be written in the following form:

$$\nu_i = \nu_i (k_r, k_s/k_r, m_y, m_x/m_y) . \quad (6)$$

In this, representation scaling on the Raman frequency for an XY_3 molecule is equivalent to fixing k_r. The values of k_r obtained through this procedure are approximately equal to those which would

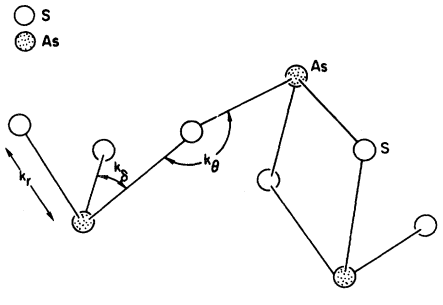

FIG. 6. Schematic representation of the local molecular order in amorphous As_2S_3. k_r, and k_δ and k_θ are, respectively, the bond-stretching, and bond-bending force constants.

TABLE II. Comparison of the calculated and experimental optic-mode frequencies.

Material	Mode	Molecular model (cm^{-1})	Infrared (cm^{-1})	Raman (cm^{-1})
As_2S_3	ν_1	344	340	344
	ν_2	162	163	···
	ν_3	310	309	···
	ν_4	133	120-150	···
As_2Se_3	ν_1	227	246	227
	ν_2	102	101	···
	ν_3	220	218	···
	ν_4	78	75	···

be estimated from the application of Gordy's rule.[27] Having obtained a procedure for estimating k_r, the only other variable in the calculation is then the ratio of bond-bending to bond-stretching force constant; this ratio is very nearly 0.1 for most pyramidal molecules.[25] Referring to Table III, the agreement between the calculated and measured frequencies is good and demonstrates the validity of a molecular model. This in turn implies that the assumption of a weak bond-bending force constant at the bridging S and Se atoms is valid. This is further substantiated by the observations of Taylor, Bishop, and Mitchell[28] which show no change in the dominant frequencies of As_2Se_3 on passing from the solid to the liquid. In our interpretation, the frequencies they have tracked are associated with the pyramidal units which are assumed to be present in both phases. In As_2S_3, the frequency of ν_4 cannot be resolved, whereas in As_2Se_3, the ν_4 frequency of this mode differs slightly in the measurements of Zlatkin and Markov[5] and Taylor, Bishop, and Mitchell.[4]

Figure 7 contains a schematic representation of the atomic motions of the optic modes in an XY_3 pyramidal molecule. In this molecule all modes are both ir and Raman active. The assignment of ir activity is based on group-theoretical considerations in which the X and Y atoms are different. If the molecule is ionic, e.g., made up of X^{3+} and Y^{-1} atoms, then there is no question regarding the ir activity. On the other hand, if the bonding is covalent, and if the atoms are similar, e.g., As and Se or As and Br, then there are questions that can be raised about the occurrence of ir activity. These questions are addressed in Sec. V, where we consider two mechanisms for ir activity.

V. INFRARED EFFECTIVE CHARGES

A. Experimental Values

As we mentioned in Sec. IV, a calculation of e_T^* from experimental data requires a knowledge of the mode mass m_i, and of N, the number of oscillators per unit volume. We equate the number of oscillators per unit volume to the number of As atoms per unit volume. The mode mass is obtained by considering the atomic displacement coordinates of the optic modes. For an XY_3 molecule, the problem is solved by Herzberg.[25] For ν_1 the mode mass m_1 is given by

$$m_1 = 3m_y m_x \sin\beta/(m_x + 3m_y \sin\beta)\,, \tag{7}$$

whereas for ν_2, ν_3, and ν_4, it is given by

$$m_{2,3,4} = 3m_y m_x \cos\beta/(m_x + 3m_y \cos\beta)\,,$$

where β is the angle between an X-Y bond and the threefold axis of symmetry of the molecule. For $AsCl_3$ and $AsBr_3$, β is 60 deg; for AsS_3 and $AsSe_3$, we also use a value of 60 deg. The value of 60 deg is consistent with the bonding in crystalline As_2S_3 and As_2Se_3. Table IV contains values of the effective-charge parameters for these chalcogenide glasses. In each case, the largest value of e_T^* is associated with ν_3, the antisymmetric stretching mode. The effective charge for ν_1, the symmetric stretching mode, is slightly smaller. Finally, the effective charges in ν_2 and ν_4, the bond-bending modes, are still smaller, but by numerical factors. Also included in the table are estimates of the effective charges for a molecule with a similar structure NF_3. These were estimated from absorption measurements[29] and normalized to 1.0 for ν_3. As in As_2S_3 and As_2Se_3, the dominant ir mode is ν_3. The ratios of the e_T^* for ν_1 and ν_3 are essentially the same in all three materials; however, ν_2 and ν_4 have substantially smaller e_T^* in NF_3. Also included in Table IV are estimates of the bond ionicity for As-S, As-Se, and N-F.

B. Theoretical Considerations

It is well known that there are both static and dynamic contributions to e_T^*.[14,15] In the simplest model, the static contribution is associated with the ionic charge on the constituent atoms. The dynamic component is due to charge redistribution (or deformation) as it occurs during the execution of an optic-mode atomic motion. In the limiting cases of completely ionic or covalent bonding, the contributions to e_T^* are, respectively, static or

TABLE III. Comparison of the calculated and experimental effective charges.

Molecular model mode	Model calculations e_T^*		Expt. e_T^*		
	Rigid ion	Charge deformation	As_2S_3 $f_i=0.06$	As_2Se_3 $f_i=0.04$	NF_3 $f_i=0.22$
ν_1	Ze	0	$1.65e$	$1.31e$	$0.6e$
ν_2	Ze	0	$0.71e$	$0.69e$	$0.07e$
ν_3	Ze	$\sim e$	$1.92e$	$1.92e$	$1.0e$
ν_4	$<$Ze	$<e$	$<0.3e$	$<0.2e$	$0.07e$

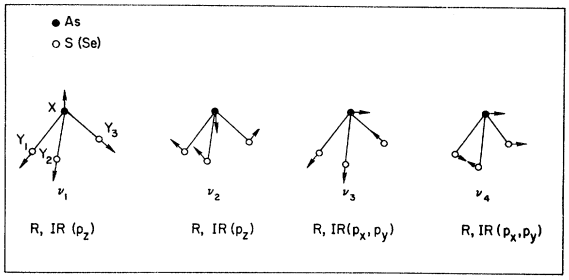

FIG. 7. Schematic representation of the normal modes of vibration of a pyramidal XY_3 molecule. R stands for Raman, IR for infrared.

dynamic. The effective charge (e_T^*) of ~ 1.0e for all of the alkali halides is very nearly all static charge,[14,30] whereas, the effective charges of the homopolar crystals trigonal Se and trigonal Te,[14] are due entirely to dynamic effects.[30] Experimentally, the values of e_T^* are similar for both classes of materials, so that it is not possible to identify the mechanism for e_T^* from its magnitude. In this regard, the effective charges of almost all of the simple eight-electron diatomic crystals $A^{8-N}B^N$, whether they crystallize in the covalent and fourfold coordinated zinc-blende (or wurtzite) lattices, or in the sixfold (or eightfold) coordinated ionic NaCl (or CsCl) lattices, are all of the order of 1.0e to 3.0e.[30]

Figure 8 contains schematic representations of the effective-charge mechanisms in ionically and covalently bound XY_2 molecules. For the ionic case, Fig. 8(a), we assume a charge of $2e$ on the X atom and $-1e$ on each of the Y atoms. We indicate the relative atomic motions for an optic mode; the X atoms move to the right with a displacement ∂r_1 and the Y atom to the left with a displacement ∂r_2. From the definition of e_T^* [Eq. (2)], it follows directly that $e_T^* = 2e$, the charge on the X atom. This is the result that one would expect. For the case of covalent bonding, we have assumed charges of $+2e$ and $+1e$ on the X and Y ions, and negative charges of $-2e$ in each bond [see Fig. 8(b)]. As in the ionic case we show the atomic motions associated with an optic-mode motion. Here we assume that electronic charge flows out of the bond under tension and into the bond under compression. If a charge of ∂e is transferred and if r_0 is a characteristic interatomic equilibrium spacing, then it follows that

$$\partial M \sim r_0\, \partial e \ . \tag{8}$$

We can obtain an estimate of $\partial e/\partial r_0$ by considering the case in which the molecule is ionized. If an X atomic core and its electron are removed and the other bond is compressed, then a charge of $-e$ is transferred for a bond length charge of r_0; therefore

$$\frac{\partial e}{\partial r_0} \sim \frac{e}{r_0} \ . \tag{9}$$

Substitution of (8) into (9) yields the result that $e_T^* \sim e$. It follows that a simple model for dynamic charge can yield values of e_T^* of the order of e. Chen and Zallen[31] considered a shell model calcula-

TABLE IV. Comparison of the effective-charge parameters for amorphous As_2S_3 and As_2Se_3 and crystalline Se and Te.

Material	e_T^*	
	Intramolecular	Intermolecular
As_2S_3	ν_3, 1.92e	ν_1, 1.65e
	ν_4, <0.3e	ν_2, 0.71e
As_2Se_3	ν_3, 1.92e	ν_1, 1.31e
	ν_4, 0.2e	ν_2, 0.69e
	Intrachain	Interchain
Trigonal Se	E, 0.8e	A_2, 0.6e
Trigonal Te	E, 2.2e	A_2, 2.3e

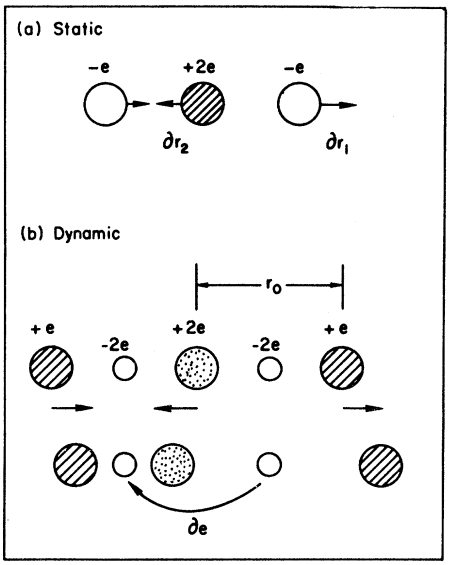

FIG. 8. Effective-charge mechanisms for XY_2 molecules: (a) Schematic representation of ionic bonding. The X atom is a positive divalent ion; each of the Y atoms is negatively charged. The arrows indicate the displacement coordinates for an optic mode. For this case the effective charge is static. (b) Schematic representation of covalent bonding. The X and Y atoms are positive cones with charges of $+2e$ and $+e$, respectively. The bonding charge ($-2e$) is located between the atoms. The arrows indicate the motions associated with an optic mode. In the lower-half of the figure, the atoms are shown in their displaced positions. The arrow there indicates a transfer of charge from the bond under tension to the bond under compression. The effective charge for this type of bonding is dynamic.

tion for trigonal Se and trigonal Te. The mechanism for e_T^*, in the A_2 mode in their model, is completely equivalent to the one discussed above.

If the bonding is partially ionic then one would expect contributions from both effects. For a bond ionicity of $f_i (\leq 1.0)$, one would expect a static contribution given by

$$e_T^*|_s \sim z e f_i , \tag{10}$$

where z is the classical chemical valence, two in our example above. In Table III, we have included values of e_T^*, as estimated for XY_3 molecules, for the two limiting cases of completely ionic and completely covalent bonding.

We now compare the calculated and experimental values for e_T^*. Before discussing the effective charges for the chalcogenide glasses, we discuss those of NF_3. In the rigid-ion model, the ratio of the e_T^* for modes ν_2 and ν_3 is expected to be of order unity; for NF_3, this ratio is 0.07. On the other hand, for a charge deformation model, a ratio close to zero is expected. These comparisons suggest that the dominant mechanism in NF_3 is dynamic. However, the situation is not so simple due to the large value of e_T^* for ν_1. In a rigid-ion model one anticipates a large e_T^*, but in a charge deformation model one anticipates a value close to zero. We therefore conclude that for NF_3, there are both static and dynamic contributions to e_T^* and that the relative contributions differ for different modes. The single-bond ionicities for As-S and As-Se bonds are substantially smaller than the NF bond ionicity. If we assume that e_T^* for ν_1 in NF_3 is due to static charge and that e_T^* for ν_3 has comparable static and dynamic contributions, then based on bond ionicities we would expect a substantially reduced ratio of these two effective charges in As_2S_3 and As_2Se_3 if the same effective-charge mechanisms were operable. The ratios are about equal in all three materials suggesting that different mechanisms are important in the amorphous solids. This is further substantiated by noting that e_T^* for ν_2 in both As_2S_3 and As_2Se_3 is very much larger than e_T^* for ν_2 in NF_3, or more precisely that the ratio of the e_T^* for ν_2 and ν_3 is very much larger. This large ratio, as well as the occurrence of values of e_T^* of order $0.2e-2.0e$ for all of the modes in As_2S_3 and As_2Se_3 is at first sight suggestive of a rigid-ion mechanism. However, the values of e_T^* for both materials are much larger than would be anticipated on the basis of the very low ionicities of As-S and As-Se bonds. If we assume that the dominant contributions to all of the modes in As_2S_3 and As_2Se_3 are dynamic, then there is no problem with the e_T^* values for ν_3 and ν_4. However, it is necessary to account for the large values of e_T^* for ν_1 and ν_2. This can be done by introducing solid-state effects which are here manifested by an intermolecular coupling mechanism. Before we present this argument, we illustrate the dyamic mechanism for e_T^* for ν_3.

In Fig. 9(a) we illustrate the intramolecular charge redistribution mechanism that leads to ir activity in ν_3. The relative displacement of As and S (or Se) atoms produces an oscillating dipole moment in either the x or y direction. In this mode two bonds are either in compression or tension with the third bond in the other state. This mode has been described by Zallen *et al.*[32] as a rigid sublattice mode. Zallen *et al.*[32] studied the ir-active modes of crystalline As_2S_3 and As_2Se_3 for geometries in which the electric field vector was parallel to the layers. They have identified the dominant ir modes in both crystalline solids and have found that they occur at very nearly the same frequencies as the dominant modes of the corresponding amorphous phases. The orientation of the pyramidal units in the crystalline materials is consistent with this explanation.

In Fig. 9(b) we indicate two linear combinations of the A_1 modes (ν_1 and ν_2). The first combination is a breathing mode with no ir activity; both bonds shown are either in compression or tension. The second combination is predominantly a bond-bending mode. The atoms execute atomic motions in the z direction. Adjacent bonds are in compression and tension, so that there is a dynamic contribution to e_T^*. Since the bond-bending force constant at the bridging S (or Se) atoms is small, the two modes shown will have frequencies that are very close to ν_1 and ν_2, respectively, of the isolated molecule. Other combinations of A_1 motions as well as disorder can lead to ir activity in ν_1.

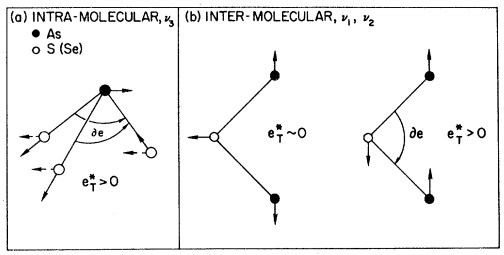

FIG. 9. Effective charge mechanisms in AsS_3 and $AsSe_3$ molecules: (a) Shown here is a representation of the effective-charge mechanism for the ν_3 mode. In this mode two bonds are in tension (or compression) and the third is in compression (or tension). The direction of charge transfer is indicated, as is the effective atomic displacement. The effective-charge mechanism is intramolecular and the polarization is in the x and y directions. (b) Shown here are two intermolecular modes. The coupling of the $AsS_3(Se_3)$ units is through the bridging S(Se) atoms. The first combination of ν_1 and ν_2 modes (Fig. 6) gives rise to a symmetric stretching mode which is only Raman active.

The argument for intermolecular coupling is reinforced by the observation the damping constants of ν_1 and ν_2 in both As_2S_3 and As_2Se_3 are about a factor of 2 larger than ν_3. The ir activity in ν_3 is clearly intramolecular. The occurrence of ir activity due to intermolecular effects has been documented in the literature.[33] Table IV gives values of e_T^* for the intra- and intermolecular modes in As_2S_3 and As_2Se_3 and for the intra- and interchain modes in trigonal Se and Te.[33] Again the magnitude of e_T^* is not sensitive to the effective-charge mechanism, i.e., whether it is static or dynamic. In trigonal Se and Te, the intra- and interchain e_T^* in each material are comparable. In amorphous As_2S_3 and As_2Se_3, the intramolecular e_T^* are larger than the intermolecular e_T^*. Furthermore, all the values of e_T^* are in the range of those also found in ionic crystals.

VI. SUMMARY

There are several points we would like to make in this summary. The first concerns the results of our new measurements of the ir reflectance. For both As_2S_3 and As_2Se_3, we find that two modes contribute to the dominant reststrahlen band. The higher-frequency mode is clearly the one that dominates the Raman scattering for a symmetric scattering geometry. The symmetry properties of these modes are consistent with the predictions of the molecular model of Lucovsky and Martin.[13] Whereas Taylor, Bishop, and Mitchell[4] invoked a Gaussian line shape to describe the dominant band in As_2Se_3, we find a skewed absorption band that is best fit by two Lorentzian modes.

In amorphous Si, it has been demonstrated[34] that the reduced ir and Raman spectra are essentially the same. This has been interpreted in terms of a disorder-incuded breakdown of selection rules[35] so that the ir and Raman data, properly normalized, reflect the density of phonon states of the material. This is clearly not the case in As_2S_3 and As_2Se_3. We have demonstrated a consistency between the reported optic-mode frequencies and their relative ir and Raman intensities, and the predictions of the molecular model.[13] Here, we wish to point out that a complete spectrum of behavior is to be expected in amorphous semiconductors. For the amorphous elemental semiconductors Si and Ge, and for the III-V materials, we cannot apply molecular models[13]; in these materials, the Raman and ir spectra are expected to bear a close correspondence to the phonon density of states of a disordered crystal.[35] Stated otherwise, a breakdown of selection rules, due to disorder, will be the dominant factor in determining ir or Raman activity. At the other end of the spectrum, there are many glasses wherein a molecular description is valid. In these materials we expect relatively strong effects due to molecular selection rules, with a weaker background due to selection rule breakdown. Examples of materials in this category are As_2S_3 and As_2Se_3, as well as fused silica and germania. Finally, there are indications that the behavior in amorphous Se and Te is intermediate between these two cases.[13,36,37]

The final point concerns the infrared effective charges. We have calculated these for both As_2S_3 and As_2Se_3 and have demonstrated that their magnitudes are not a manifestation of a large ionic contribution to the bonding, as had been suggested by others.[5] The magnitudes of e_T^* are consistent with a charge deformation model in which the effective charge is dynamic and due to a charge redistribution between adjacent bonds which are in compression and tension. This point is reinforced by comparing the values of e_T^* for As_2S_3 and As_2Se_3 with those reported for trigonal Se and trigonal Te. In the case of the homopolar materials, there are no ionic contributions to e_T^*; all of the effective charge is dynamic and due to redistribution and deformation effects.[14]

ACKNOWLEDGMENTS

The author wishes to express his appreciation to M. McClure, M. Myers, H. Six, and D. Thornburg for their assistance with many of the experimental aspects of this work, and to R. M. Martin and F. Galeener for valuable discussions and critical reading of the manuscript.

[1]A. R. Hilton, C. E. Jones, R. D. Dobratt, H. M. Klein, A. M. Bryant, and T. D. George, Phys. Chem. Glasses 7, 116 (1966).

[2]E. J. Felty, G. Lucovsky, and M. B. Myers, Solid State Commun. 5, 555 (1967).

[3]G. Lucovsky, M. H. Brodsky, and E. Burstein, in *Localized Excitations in Solids*, edited by R. F. Wallis (Plenum, New York, 1968), p. 592.

[4]P. C. Taylor, S. G. Bishop, and D. L. Mitchell, Solid State Commun. 8, 1783 (1970).

[5]L. B. Zlatkin and Ye. F. Markov, Phys. Status Solidi 4(a), 391 (1971).

[6]M. Onomichi, T. Arai, and K. Kudo, J. Non-Cryst. Solids 6, 362 (1971).

[7]A. T. Ward and M. B. Myers, J. Phys. Chem. 73, 1374 (1969).

[8]R. J. Kobliska and S. Solin, J. Non-Cryst. Solids 8–10, 191 (1971).

[9]J. Schottmiller, M. Tabak, G. Lucovsky, and A. Ward, J. Non-Cryst. Solids 4, 80 (1970).

[10]G. Lucovsky, Bull. Am. Phys. Soc. 17, 113 (1972).

[11]I. G. Austin and E. S. Garbett, Phil. Mag. 23, 17 (1971).

[12]R. J. Bell, N. F. Bird, and P. Dean, J. Phys. C 1, 299 (1968).

[13]G. Lucovsky and R. M. Martin, J. Non-Cryst. Solids

8–10, 185 (1971).
[14]E. Burstein, M. H. Brodsky, and G. Lucovsky, Intern. J. Quantum Chem. 15, 759 (1967).
[15]E. Burstein, J. Phys. Chem. Solids Suppl. 21, 315 (1965).
[16]H. W. Verleur, J. Opt. Soc. Am. 58, 1356 (1968).
[17]R. Shuker and R. W. Gammon, Phys. Rev. Letters 25, 222 (1970).
[18]R. J. Kobliska and S. Solin (unpublished).
[19]P. C. Taylor, S. G. Bishop, and D. L. Mitchell, in *Phonons*, edited by M. A. Nusimovici (Flammarion, Paris, 1971), p. 197.
[20]A. T. Ward (unpublished).
[21]E. Burstein, A. Pinczuk, and R. F. Wallis, in *Proceedings of the Conference on the Physics of Semimetals and Narrow Gap Semiconductors*, edited by D. L. Carter and R. T. Bate (Pergamon, New York, 1971), p. 251.
[22]G. Su and J. Bock, Office of Naval Research Report No. Nonr-668(19), 1968, p. 27 (unpublished).
[23]G. Su and B. T. Chen, Office of Naval Research Report No. Nonr-668(19), 1968, p. 33 (unpublished).
[24]N. Morimoto, Mineral. J. (Sapporo) 1, 160 (1954); A. A. Vaipolin, Sov. Phys. Crystal. 10, 509 (1966).
[25]G. Herzberg, *Infrared and Raman Spectra of Polyatomic Molecules* (Van Nostrand–Reinhold, New York, 1945).
[26]K. Nakamoto, *Infrared Spectra of Inorganic and Coordination Compounds* (Wiley, New York, 1963).
[27]W. Gordy, J. Chem. Phys. 14, 305 (1946).
[28]P. C. Taylor, S. G. Bishop, and D. L. Mitchell, Phys. Rev. Letters 27, 414 (1971).
[29]E. L. Pace and L. Pierce, J. Chem. Phys. 23, 1248 (1955).
[30]G. Lucovsky, R. M. Martin, and E. Burstein, Phys. Rev. B 4, 1367 (1971).
[31]I. Chen and R. Zallen, Phys. Rev. 173, 833 (1968).
[32]R. Zallen, M. L. Slade, and A. T. Ward, Phys. Rev. B 3, 4257 (1971).
[33]G. Lucovsky, Phys. Status Solidi 49(b), 633 (1972).
[34]J. E. Smith, Jr., Bull. Am. Phys. Soc. 17, 136 (1972).
[35]J. E. Smith, Jr., M. H. Brodsky, B. L. Crowder, M. I. Nathan, and A. Pinzcuk, Phys. Rev. Letters 26, 642 (1971).
[36]G. Lucovsky, in *Physics of Selenium and Tellurium*, edited by W. C. Cooper (Pergamon, Oxford, 1969), p. 255.
[37]G. Lucovsky, A. Mooradian, W. Taylor, G. B. Wright, and R. C. Keezer, Solid State Commun. 5, 439 (1967).